MADRID
inter.noise 2019
June 16 - 19
NOISE CONTROL FOR A BETTER ENVIRONMENT

Analysis of drum brake defects as a source of automotive vibro-acoustics

Ramesh, Ananthapadmanabhan[1]
Indian Institute of Technology Tirupati
Tirupati
Andhra Pradesh
517506

Sundar, Sriram[2]
Indian Institute of Technology Tirupati
Tirupati
Andhra Pradesh
517506

ABSTRACT

Drum brakes are one of the major sources of disturbances that cause high frequency vibro-acoustic problems in automotive such as cars, buses, and trucks. The forces generated at the pivots of the brake shoes cause disturbances (to the automotive system), which are more influenced if there are inherent defects in the brake system, such as asymmetry in the brake shoes. Hence, the objective of this work is to develop an analytical model that predicts these forces, which are used to quantify the influence of drum brake shoe defects on automotive vibration. A four degree-of-freedom (DoF) contact mechanics based vibration model has been developed to simulate the braking event. For a typical automotive brake, the time-domain results showed that even for a minor asymmetry in the brake shoes, there was an appreciable change in the amplitude of disturbance. It is envisioned that this research will throw light on the contribution of brake defects towards cabin noise and eventually help in developing accurate vibro-acoustic based drum brake health monitoring systems.

Keywords: Drum brake noise, Contact mechanics, Brake defect
I-INCE Classification of Subject Number: 11, 41, 76

[1]me17ms001@iittp.ac.in
[2]sriram@iittp.ac.in

1. INTRODUCTION

Automotive brakes are usually analysed for their performance assuming they are devoid of any defects [1], [2] and [3]. Nonetheless, defects are bound to occur in drum and disc brakes due to manufacturing tolerances and continuous usage. Drum brakes are indispensable in automotive applications due to their reliable performance, compact structure, higher braking power and ease of parking brake installment [4]. Defects in drum brakes can have influence not only on the performance and life of the brakes but also on the safety and noise-vibration-harshness (NVH) characteristics of the vehicle. Since these have a direct influence on the cost and the statutory requirements [5] that govern the automotive industry, analysis of defects in drum brakes is essential.

Defects in the drum brakes can be broadly classified into kinematic defects (related to geometry) and dynamic defects (related to actuation force/pressure). Out of roundness of the drum, drum surface crack [6], drum surface waviness and asymmetry of the brake shoes are some common examples of kinematic defects. Delay in actuation, lower actuation pressure and transience in actuation pressure are some possible dynamic defects. All the forces produced at the pivot point of the shoe will be transferred to chassis through the backing plate and will lead to vibro-acoustic source. The work presented here focuses on the asymmetry of the brake shoes and actuation force and its influence on the force transmitted to chassis through pivot point of the brakes using the analytical model, in time domain analysis. This force is one of the major sources of vibro-acoustic noise in the cabin during braking.

2. PROBLEM FORMULATION

To study the dynamics during the braking event an analytical model was developed for the system shown in Fig.1. The drum of the drum brake was connected to a flywheel with high mass moment of inertia (I_f) using torsional stiffness (K_s) and torsional damper (C_s). The inertia of the flywheel represents the portion of inertia of automotive which a single brake is trying to stop during a braking event. The torsional stiffness and damper represent equivalent stiffness and damping of the components between the wheel and the brake. This forms a 4 degree-of-freedom (DoF) system with rotational DoF for the flywheel (θ_f), brake drum (θ_d), left brake shoe (θ_l) and right brake shoe (θ_r) as shown in the Fig.1. The contact point between the brake drum and the shoe was calculated geometrically, while the contact was represented by Kelvin - Voigt model with linear contact stiffness and viscous contact damper [7].

2.1 Analytical model

The braking event was simulated by giving an initial angular velocity to the flywheel (representative of the part of the vehicle′s kinetic energy dissipated by one brake) and the drum. Then the actuation forces (F^e) were applied as external forces to the tip of the brakes shoes which in turn rotates about the pivot point O_l and O_r and made contact with the drum producing the necessary braking torque for the drum and flywheel to stop. The key assumptions in the proposed analytical model were: (i) Smoothened Coulomb friction model was used to represent the sliding friction between brake shoe and drum; (ii) Contact forces between brake shoe and drum was modeled by Hertzian Contact theory.

Using Newton's law, equations of motion were derived for the DoFs as given below:

$$I_f\ddot{\theta}_f + C_s(\dot{\theta}_f - \dot{\theta}_d) + K_s(\theta_f - \theta_d) = 0 \tag{1}$$

$$I_d\ddot{\theta}_d + C_s(\dot{\theta}_d - \dot{\theta}_f) + K_s(\theta_d - \theta_f) = \tau_d \tag{2}$$

$$I_l\ddot{\theta}_l + F_l^n d_l - F_l^f h_l = F_l^e q_l \tag{3}$$

$$I_r\ddot{\theta}_r + F_r^n d_r + F_r^f h_r = F_r^e q_r \tag{4}$$

Here, I_f and I_d represent the mass moments of inertia of flywheel and drum about the axis of rotation respectively. Similarly, I_l and I_r represent the mass moments of inertia of left and right shoe about the axis of rotation. The moment arm of F^n and F^f about O was represented as d and h. In th same way, the moment arm of actuation force (F^e) was represented by q. Braking torque (τ_d) given by

$$\tau_d = -(F_l^f + F_r^f)R_d \tag{5}$$

where R_d is the radius of the drum. Normal force (F^n) produced at the point of contact between left and right shoe with the drum was given by Eqn.(6) and Eqn.(7), where ε represents the indentation between the brake shoe and drum.

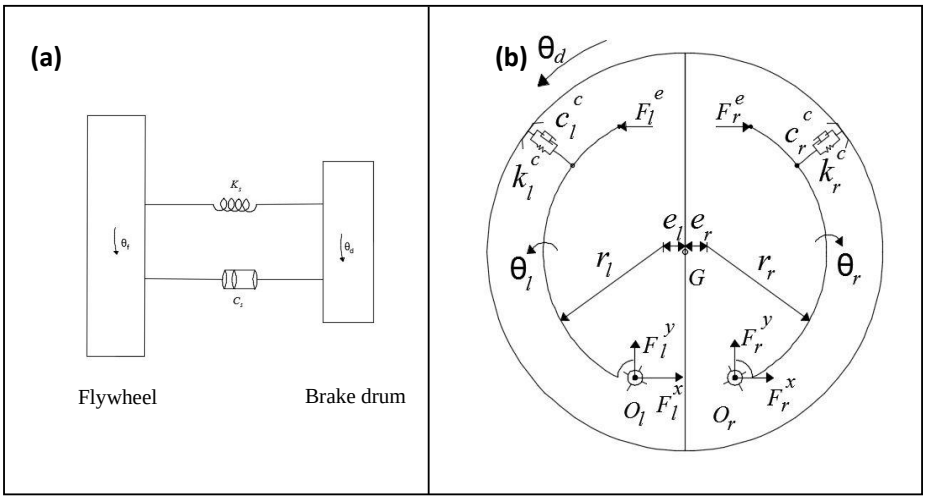

Figure 1: Analytical model of system explained in section 1: (a) Front view showing the flywheel and drum brake arrangement; (b) Expanded side view of drum brake, showing internal components

$$F_l^n = k_l^c\varepsilon_l + c_l^c\dot{\varepsilon}_l \tag{6}$$

$$F_r^n = k_r^c\varepsilon_r + c_r^c\dot{\varepsilon}_r \tag{7}$$

Linear contact stiffness was defined for a line contact based on Hertzian contact theory [7] as given by Eqn.(8).

$$k^c = \frac{\pi}{4}E_{eq}l^c. \tag{8}$$

Here E_{eq} is equivalent Young's modulus given by Eqn.(9), where υ_d and υ_s are Poisson's ratio for drum and shoe,respectively. Likewise, E_d and E_s represents Young's modulus of brake drum and shoe.

$$E_{eq} = \left[\frac{1 - \upsilon_d^2}{E_d} + \frac{1 - \upsilon_s^2}{E_s} \right]^{-1} \tag{9}$$

3. DYNAMIC ANALYSIS

The differential equations of motion given from Eqn.(1) to Eqn.(4) were numerically integrated to obtain the system response to the excitation force. Initially, both the shoes were oriented at the same angle and the pivot location of both shoes was located at equal distance from the centre of the drum. For analysis, a typical automobile of mass 1000 kg traveling at 100 km/hr was considered and parameters were calculated as shown in Table 1. Different system responses were estimated during dynamic analysis like the angular displacement of brake shoes, the angular velocity of drum and flywheel, normal force at the point of contact, indentation of brake shoes. The entire analysis was confined to time domain. From automobile NVH perspective, the resultant reaction force at O is critical because these forces would be transferred to the chassis through the backing plate which would lead to unwanted vibrations of the vehicle and hence becoming a vibro-acoustic source.

Table 1: *Parameters obtained from a typical automobile of 1000 kg, as discussed in section 3*

Parameters	Values
I_f	17.1 kg.m^2
I_d	0.041 kg.m^2
R_d	180 mm
K_s	1835 N/rad
C_s	5 N.s/rad

Braking force was applied after 0.2s from the beginning of the simulation and ramped up to a maximum value in 0.5 s to simulate a practical case of a braking event. Fig.2 explains the variation of the resultant reaction force at O with respect to time in the symmetric case and T denotes the time between successive impacts. It is evident from Fig.2 that the whole braking event is divided into two major regimes, namely impacting regime and contact regime. For analysis, an initial angular velocity of 103.5 rad/s (equivalent to 100 km/hr) was given to both flywheel and brake drum.

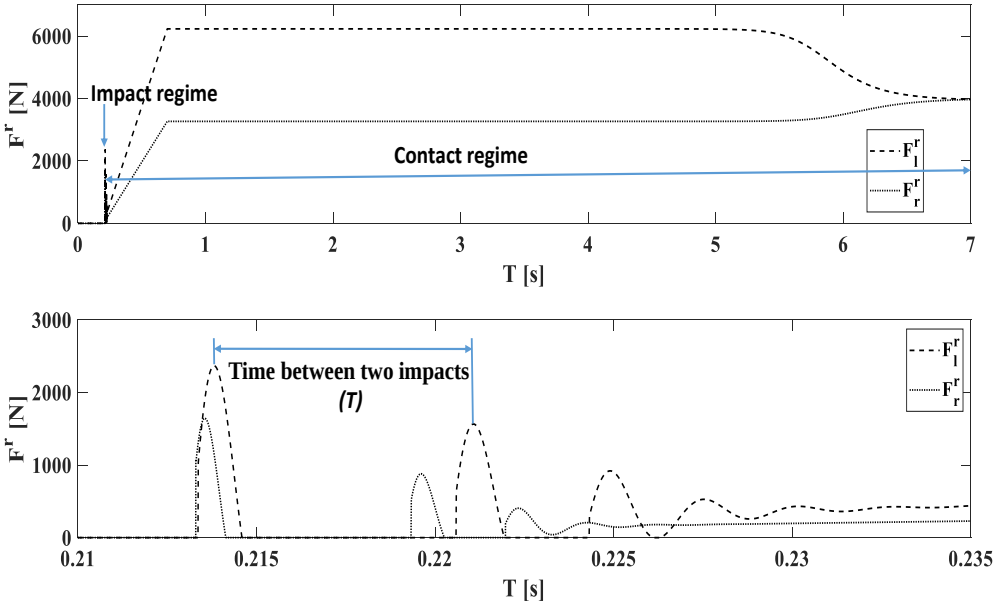

Figure 2: Reaction forces at the pivots during the braking event: (a) Full time history till drum stops rotating (b) Response focusing on the impact regime only

The magnitude of F_l^r and F_r^r in contact regime ramp up and remain constant till the drum is decelerating. F_l^r and F_r^r are equal when the w_{drum} reduces to zero. Since F^f approaches zero as w_{drum} reaches zero, the difference between F_l^r and F_r^r also tends to zero. Fig.2 indicates that the F_l^r is higher when compared to the F_r^r and this is because of the self-energizing effect in the leading shoe (left shoe in this case). Fig.3 explains the deceleration of the drum with respect to time and the stopping time is estimated to be 6.6s.

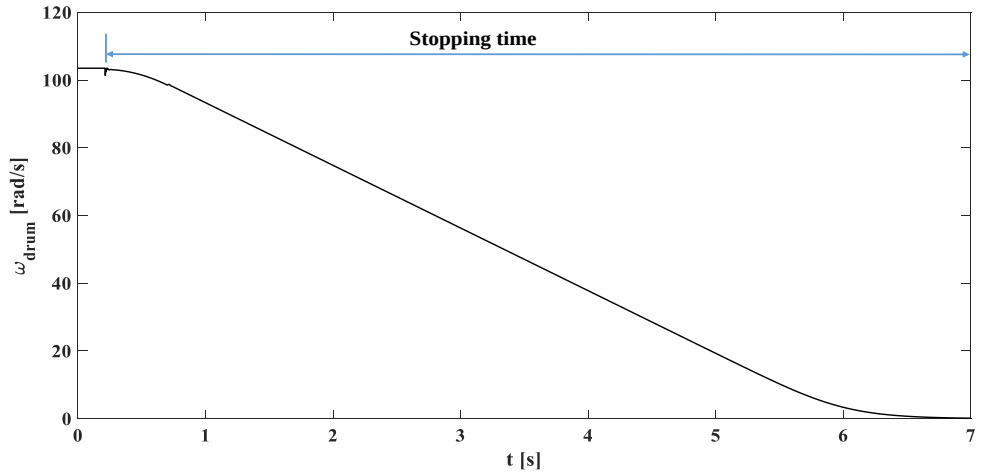

Figure 3: Time history of ω_{drum} during a typical braking event

4. INFLUENCE OF THE ASYMMETRY IN BRAKE SHOE

Any deviation from the symmetric conditions was considered as a defect due to asymmetry. From Fig.2b, it is visible that impacts were present in impacting regime and there was a drastic change in the reaction forces in a symmetric condition which leads to undesirable vibration. Since impacting regime was significant from the noise perspective, the system response in this regime is presented here.

4.1 Asymmetry with respect to the location of the pivot point of the brake shoes

Cases 1 and 2 explain the asymmetric condition when the left shoe pivot point is close and away from the brake drum when compared to the symmetric condition. From Fig.4a, it can be noted that when p_l increased (case 1), its impacts would start before the symmetric case, and since the F_l^e was a ramp from 0.2 to 0.7s, its peak value would be less (42 N) in case 1 when compared to symmetric case (56 N) during the first impact. As a result, ε_l would decrease which in turn decreases F_l^n and F_l^r. Moreover, T_l decreased which increases the frequency of impacts. As seen from Table 2, even for 3% increase in p_l, maximum amplitude of F_l^r decreased by 43% during the first impact. On the contrary, when p_l decreased (case 2) there was an increase in the F_l^r and T_l in the impact regime. From Fig.4b, it was observed that for any change in p_l, there was no change in the F_r^r and T_r.

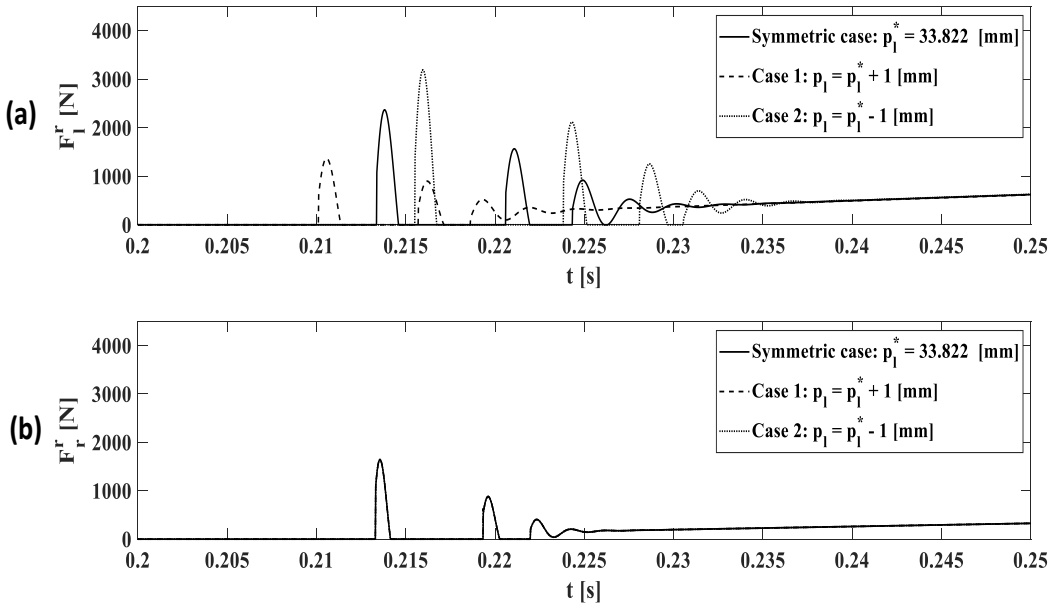

Figure 4: Time history of (F^r) in the impacting regime for asymmetry cases 1 and 2: (a) F_l^r (b) F_r^r

Cases 3 and 4 explain the asymmetric condition when the right shoe pivot point is close and away from the brake drum when compared to the symmetric case. From Fig.5b, it was observed that when p_r increased (case 3), there was a decrease in the value of F_r^r and T_r in the impact regime. Conversely, when p_r decreased (case 4) by 3%, there was an increase in the peak amplitude of F_r^r by 35% and T_r by 14.75% during the first impact.

Reason for the change in F_r^r and T_r is the same as explained in cases 1 and 2. From Fig.5a, it was observed that, for any change in p_r, there was no change in the F_l^r and T_l.

Table 2: *Percentage change in F^r and T due to asymmetry: (a) Asymmetry in left shoe (b) Asymmetry in right shoe*

Case	Parameter responsible for asymmetry	Error	% change of maximum amplitude of F_l^r w.r.t symmetric case	% change of T_l w.r.t symmetric case
1	p_l	+3%	-43	-23.6
2	p_l	-3%	+35	+13.7
5	θ_l	-2°	+79.7	+39.3
7	F_l^e	+10%	+11.1	0

Case	Parameter responsible for asymmetry	Error	% change of maximum amplitude of F_r^r w.r.t symmetric case	% change of T_r w.r.t symmetric case
3	p_r	+3%	-42	-23.3
4	p_r	-3%	+35	+14.8
6	θ_r	-2°	+80.3	+32.8
8	F_r^e	+10%	+9.5	0

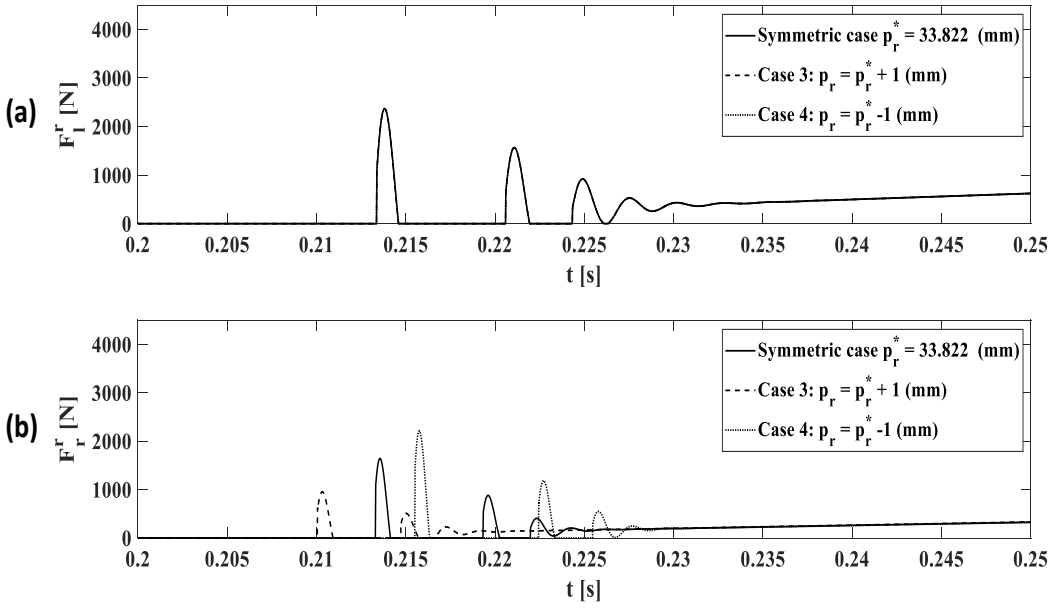

Figure 5: Time history of (F^r) in the impacting regime for asymmetry cases 3 and 4: (a) F_l^r (b) F_r^r

4.2 Asymmetry with respect to the initial orientation of the brake shoes

In symmetric condition, initial angular orientation of both shoes would be same ($\theta_l^0 = \theta_r^0 = 0°$) and there were chances of error during the assembly or manufacturing process which would lead to an unequal angular position for both shoes. Cases 5 and 6 describe

the asymmetric condition when the left and right shoe were initially oriented by an angle of 2°towards the centre of drum. From Fig.6a it was evident that when the left shoe is tilted by a 2°towards the centre of the drum (case 5), there was a drastic increase in the peak amplitude of F_l^r by 79.7% and T_l by 39.4% during the first impact. In addition, the graph of the symmetric case and case 6 were overlapping, which shows that there was no change in F_r^r and T_r by changing the left shoe initial orientation. From Fig.6b, it is clear that if the right shoe was tilted by a small angle of 2°towards the drum centre (case 6), there was a remarkable increase in the peak amplitude of F_r^r by 80.3% and T_r by 32.8% during the first impact. Moreover, the graph of the symmetric case and case 5 were overlapping, which infers that there was no change in the F_l^r and T_l after changing the initial angular orientation of the right shoe.

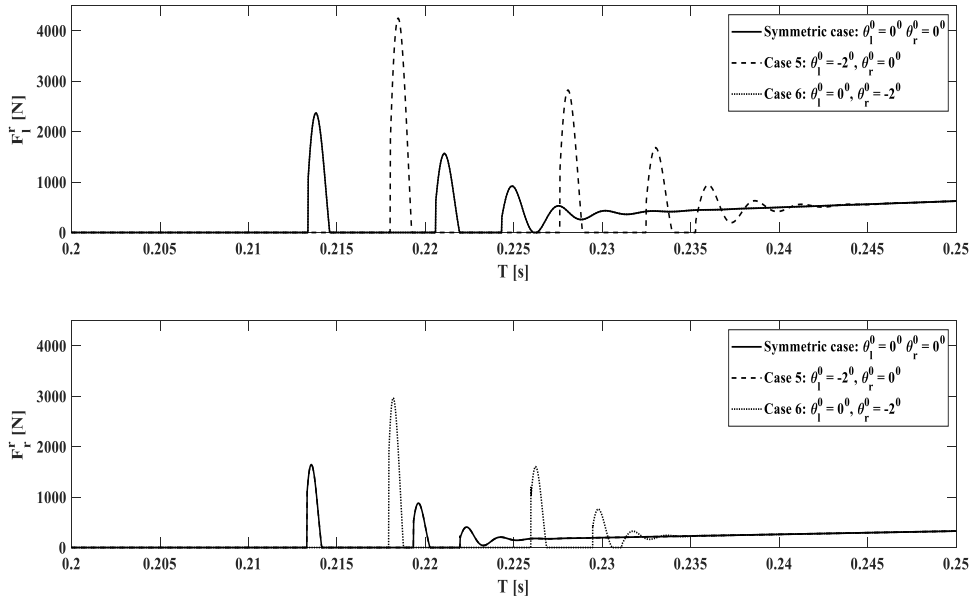

Figure 6: Time history of (F^r) in the impacting regime for asymmetry cases 5 and 6: (a) F_l^r (b) F_r^r

4.3 Asymmetry with respect to the excitation force

Normally, F_l^e and F_r^e applied at the tip of the shoes were same and due to some defects, there were chances of varying excitation force applied. Cases 7 and 8 analyse the disparity of F_l^r and F_r^r due to change in the actuating force (keeping the sum of F_l^e and F_r^e as constant). In both cases, there was no significant change in F_l^r and F_r^e during the impact regime, hence main focus was towards contact regime. From Fig.7a, it is evident that if the F_l^e was increased by 10%, there was an increas in the peak amplitude of F_l^r by 11.1% during the first impact. Correspondingly, Fig.7b shows that when F_r^e was increased by 10%, there was an increase of F_r^r by 9.5% during the first impact.

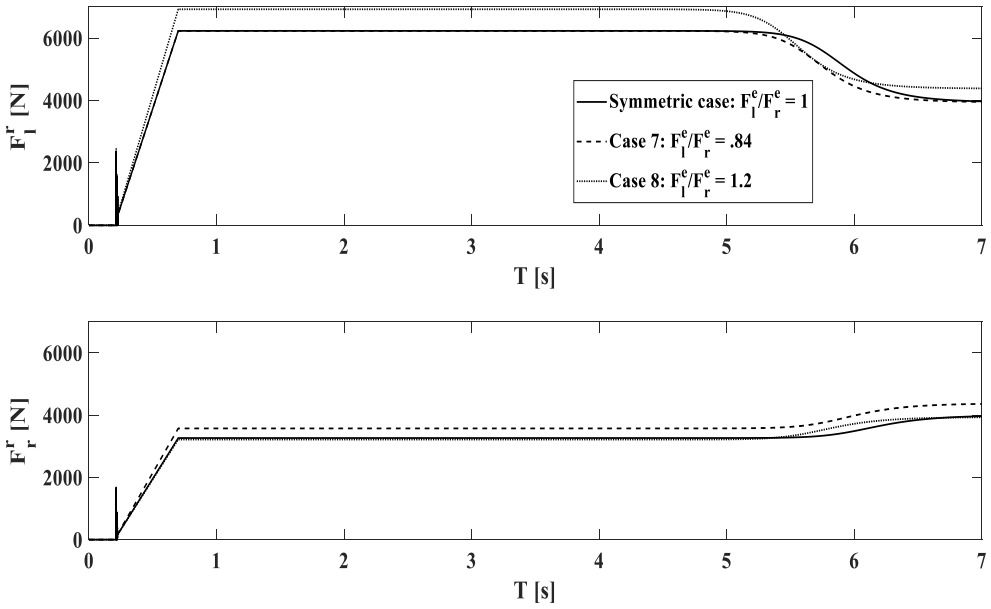

Figure 7: Time history of (F^r) for asymmetry cases 7 and 8: (a) F_l^r (b) F_r^r

5. SUMMARY

This paper investigates the effects of asymmetry of brake shoes and actuation force on the dynamic performance of the brakes. An analytical model with 4 DoF was developed and time domain analysis was performed. The analysis showed that even for a small deviation from the symmetric condition, there was a drastic change in the resultant reaction forces, which finally transmits to the chassis and leads to the source of vibro-acoustic. Counter-intuitively, all the asymmetries did not increase the reaction force at the pivot point and analysis showed that if the shoe was pivoted near the drum, reaction forces in impact regime would decrease. In future, this work can be extended to 5 Dof by including backing plate and study of other defects such as out of roundness of drum as well as surface waviness of drum and its effect on acoustics.

6. REFERENCES

[1] Huang, J., Krousgrill, C. M. & Bajaj, A. K. Modeling of automotive drum brakes for squeal and parameter sensitivity analysis. *Journal of Sound and Vibration* **289**, 245–263 (2006).

[2] Teoh, C.-Y., Ripin, Z. M. & Hamid, M. N. A. Analysis of friction excited vibration of drum brake squeal. *International Journal of Mechanical Sciences* **67**, 59–69 (2013).

[3] Ioannidis, P., Brooks, P. C. & Barton, D. C. Drum brake contact analysis and its influence on squeal noise prediction. Tech. Rep., SAE Technical Paper (2003).

[4] Zhou, M., Wang, Y. & Huang, Q. Study on the stability of drum brake non-linear low frequency vibration model. *Archive of Applied Mechanics* **77**, 473–483 (2007).

[5] Kinkaid, N., O'Reilly, O. M. & Papadopoulos, P. Automotive disc brake squeal. *Journal of sound and vibration* **267**, 105–166 (2003).

[6] Amorim, G. B., Villani, A. d. P. G. & Lopes, L. C. R. Effect of design geometry on the thermal fatigue strength of brake drum made in vermicular cast iron. Tech. Rep., SAE Technical Paper (2006).

[7] Johnson, K. L. Contact mechanics. *Cambridge university press* (1987).

[8] Sen, O. T., Dreyer, J. T. & Singh, R. Order domain analysis of speed-dependent friction-induced torque in a brake experiment. *Journal of Sound and Vibration* **331**, 5040–5053 (2012).

[9] Huang, Y. M. & Shyr, J. On pressure distributions of drum brakes. *ASME Journal of Mechanical Design* **124**, 115–120 (2002).